

Supporting Information

In situ generated catalyst: Copper (II) oxide and Copper (I) supported on $\text{Ca}_2\text{Fe}_2\text{O}_5$ for CO oxidation

Bartosz Penkala^{a,b}, Suresh Gatla^c, Daniel Aubert^a, Monica Ceretti^b, Caroline Tardivat^a, , and Werner Paulus*^b and Helena Kaper*^a

^a Ceramic Synthesis and Functionalization Laboratory, UMR 3080, CNRS/Saint-Gobain CREE, 550, Ave Alphonse Jauffret, 84306 Cavaillon, France

^b Institut Charles Gerhardt Montpellier, UMR 5253 CNRS-UM-ENSCM, Université de Montpellier, Place Eugène Bataillon, F-34095 Montpellier Cedex 5, France

^c ESRF – The European Synchrotron, 71, avenue des Martyrs, 38000 Grenoble, France

*Correspondence: helena.kaper@saint-gobain.com and werner.paulus@univ-montp2.fr.

Contents

• CO oxidation curves of reference samples	2
• Stability test of impregnated and one pot sample	2
• Surface properties derived from XPS	3
• Lattice Parameter of one pot samples	3
• XRD pattern of one pot samples as-synthesized and after reaction	4
• X-Ray analysis of as-synthesized 40Cu-CFO_OP and after reaction, compared to reference compounds	7
• Lattice Parameter of impregnated samples	7
• Figure SI 5 XRD pattern of impregnated samples as-synthesized and after reaction	9
• Fourier Transformation of the EXAFS signal of 30Cu-CFO_OP at the Cu edge	11
• Fourier Transformation of the EXAFS signal of 30Cu-CFO_OP at the Fe-edge	12
• Fourier Transformation of the EXAFS signal of 40Cu-CFO_OP at the Cu-edge	13
• Fourier Transformation of the EXAFS signal of 40Cu-CFO_OP at the Fe-edge	13

CO oxidation curves of reference samples

Fig. SI1 shows the CO oxidation curves of pure CuO prepared the same manner as the supported CuO samples and CuO deposited on γ -Al₂O₃. For comparison, the best impregnated and one-pot catalysts are added (40Cu_CFO_OP_H₂ and 40Cu_CFO_IP). The graphs shows that the CuO supported on CFO converts CO at lower temperatures than unsupported CuO (SSA: 1m²/g) or γ -Al₂O₃ (156 m²/g) as support.

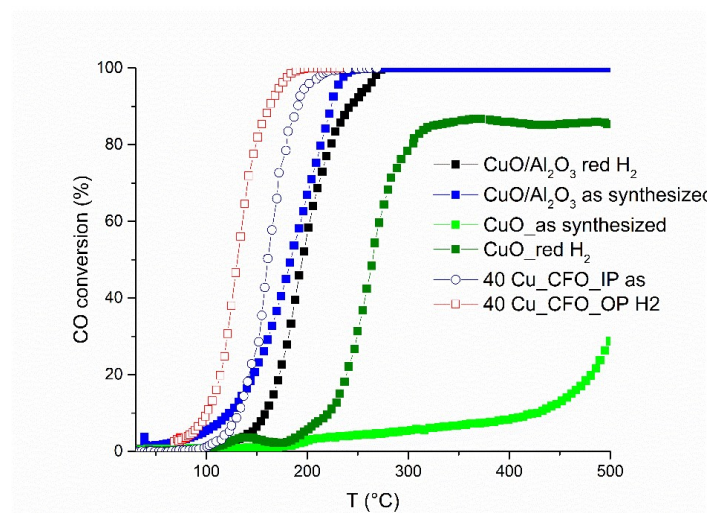


Fig. SI 1: CO oxidation light-off curves of CuO supported on Al₂O₃ and Ca₂Fe₂O₅.

Stability test of impregnated and one pot sample

Fig. SI 2 shows the CO conversion for 40Cu_CFO_IP and 40Cu_CFO_OP after hydrogen pretreatment and one light-off curve at 200°C for 24h. The test conditions were 20 mg of sample diluted in SiC,

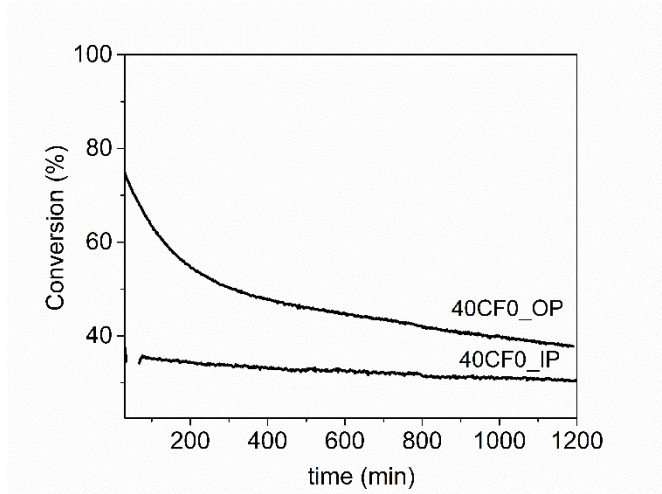


Fig. SI 2: Stability test of 40CFO_0P and 40CFO_IP. Test conditions: 20 mg of sample diluted in 300 mg of SiC, pretreatment at 300°C for 2h under 40%H₂/He, one light-off curve (2000ppm, 10000ppm O₂) and isotherm at 200°C, 2000 ppm of CO and 10000 ppm of O₂.

Surface properties derived from XPS

Table SI 1

Catalyst	$\text{Cu}2p_{3/2}$	surface composition (at% Cu) ^a	I_{ss}/I_{pp}
40_CFO_IP	933.5	24	0.45
40_CFO_IP after CO ox	933.3	23	0.33
40_CFO_OP	933.3	19	0.33
40_CFO_OP_after CO ox	933.5	16	0.41

^aThe surface compositions of Cu was calculating omitting C and O contributions, as the surface is polluted with carbonates. These values have thus a mere comparative purpose and are not absolute values.

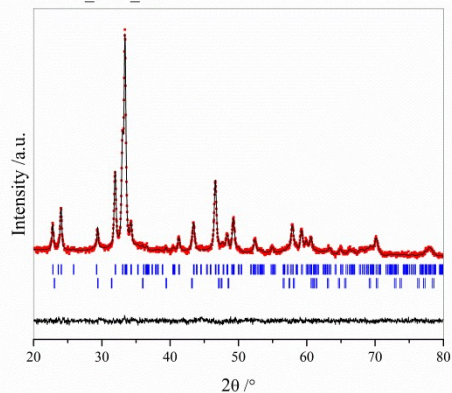
Lattice Parameter of one pot samples

Table SI 2 Refined parameters corresponding to the XRD data presented in **Fig. 4** for xCu-CFO_OP, (where $5 < x < 50$) catalysts as synthetized and after CO oxidation.

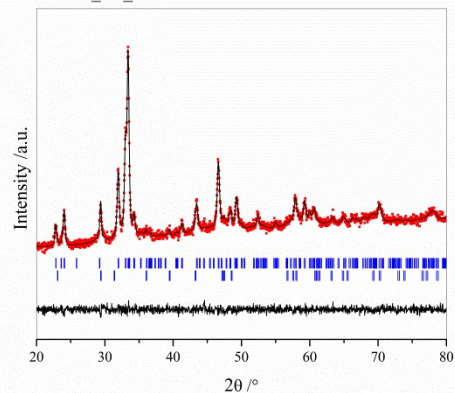
Ca ₂ Fe ₂ O ₅	P n m a	5.4231(15)	14.7830(30)	5.5972(14)	448.758(198)	97.19 (90)	1.21
CaCO ₃	R -3 c	4.9897(9)	4.9897(9)	17.0947(35)	368.583(117)	2.81 (39)	
10 Cu-CFO_OP							
Ca ₂ Fe ₂ O ₅	P n m a	5.4167(8)	14.7955(23)	5.5921(9)	448.166(119)	98.21(89)	1.46
CaCO ₃	R -3 c	4.9854(7)	4.9854(7)	17.0894(32)	368.431(134)	1.79(85)	
10 Cu-CFO_OP H2_CO							
Ca ₂ Fe ₂ O ₅	P n m a	5.42634(4)	14.8002(15)	5.6018(9)	449.893(61)	96.98(80)	1.19
CaCO ₃	R -3 c	4.9889(5)	4.9889(5)	17.0960(21)	368.431(134)	3.02(19)	
20 Cu-CFO_OP							
Ca ₂ Fe ₂ O ₅	P n m a	5.4154(3)	14.8248(8)	5.5938(3)	449.085(41)	82.46(68)	
CaCO ₃	R -3 c	4.9809(9)	4.9809(9)	17.1352(35)	368.165(117)	10.54(39)	1.16
CuO	C 2/c	4.6912(14)	3.4248(8)	5.1367(16)	81.397(41)	6.99(25)	
20 Cu-CFO_OP H2_CO							
Ca ₂ Fe ₂ O ₅	P n m a	5.4135(2)	14.7939(53)	5.5912(20)	447.786(280)	73.80(1.23)	
CaCO ₃	R -3 c	4.9795 (10)	4.9795(10)	17.0791(38)	366.753(133)	17.57(65)	1.16
CuO	C 2/c	4.6867(74)	3.4285(45)	5.1285(83)	81.269(211)	3.95(25)	
30 Cu-CFO_OP							
Ca ₂ Fe ₂ O ₅	P n m a	5.4141 (5)	14.8022(14)	5.5900(5)	447.986(75)	52.02(9)	
CaCO ₃	R -3 c	4.9862(5)	4.9862(5)	17.1147(21)	368.514(71)	35.54(48)	2.70
CuO	C 2/c	4.6932 (15)	3.4277(8)	5.1225(13)	81.200(37)	12.44(22)	
30 Cu-CFO_OP H2_CO							
Ca ₂ Fe ₂ O ₅	P n m a	5.4344(19)	14.82448(535)	5.6091(20)	451.884(280)	63.24(1.23)	
CaCO ₃	R -3 c	4.9833(10)	4.9833(10)	17.1079(38)	367.645(133)	30.44(65)	1.36
CuO	C 2/c	4.6913(74)	3.4290(46)	5.1310 (83)	81.817(211)	6.32(25)	
40 Cu-CFO_OP							
Ca ₂ Fe ₂ O ₅	P n m a	5.4143(8)	14.8247(22)	5.5922(8)	448.865(114)	50.95(32)	
CaCO ₃	R -3 c	4.9872(6)	4.9872(6)	17.1230 (22)	368.830(78)	31.90(32)	1.92
CuO	C 2/c	4.68828 (101)	3.42443(73)	5.14093(104)	81.412(30)	17.15(19)	
40 Cu-CFO_OP H2_CO							
Ca ₂ Fe ₂ O ₅	P n m a	5.4251(4)	14.8102(11)	5.6035(4)	450.113(60)	46.64(90)	
CaCO ₃	R -3 c	4.9887(3)	4.9887(3)	17.1107(15)	368.536(50)	40.12(90)	1.72
CuO	C 2/c	4.6839(72)	3.4237(39)	5.1405(82)	81.501(158)	13.2490)	
50 Cu-CFO_OP							
Ca ₂ Fe ₂ O ₅	P n m a	5.4165(3)	14.8386(10)	5.5927(4)	449.506(52)	48.54(42)	
CaCO ₃	R -3 c	4.9877(4)	4.9877(3)	17.1182(15)	368.797(49)	30.13(31)	1.92
CuO	C 2/c	4.6901(7)	3.4221(5)	5.1345(7)	81.281(20)	21.33(27)	

XRD pattern of one pot samples as-synthesized and after reaction

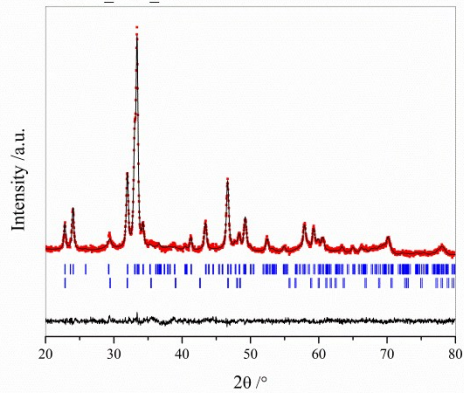
C. 5Cu_CFO_OP



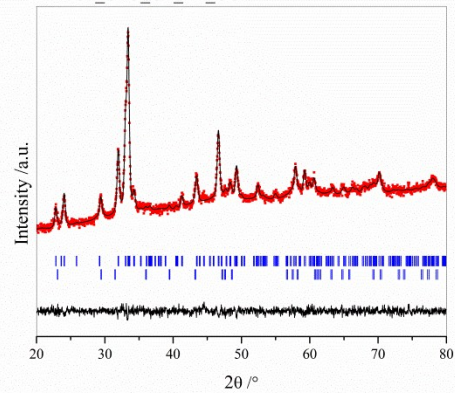
D. 5Cu_H2_CO



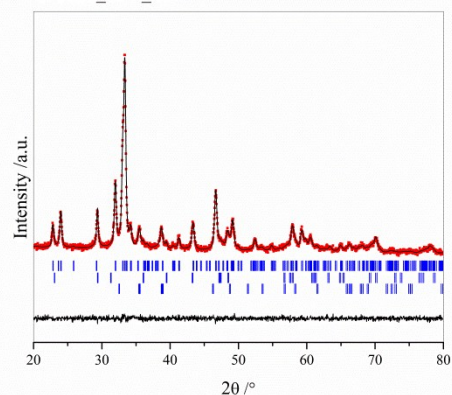
E. 10Cu_CFO_OP



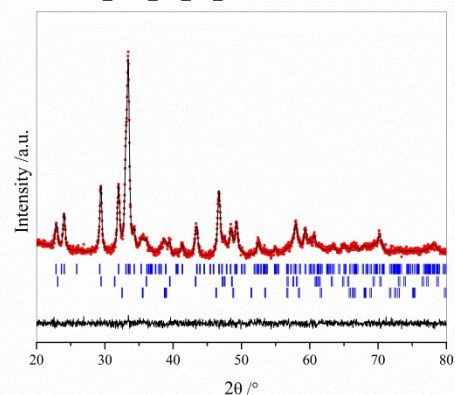
F. 10Cu_CFO_OP_H2_CO



G. 20Cu_CFO_OP



H. 20Cu_CFO_OP_H2_CO



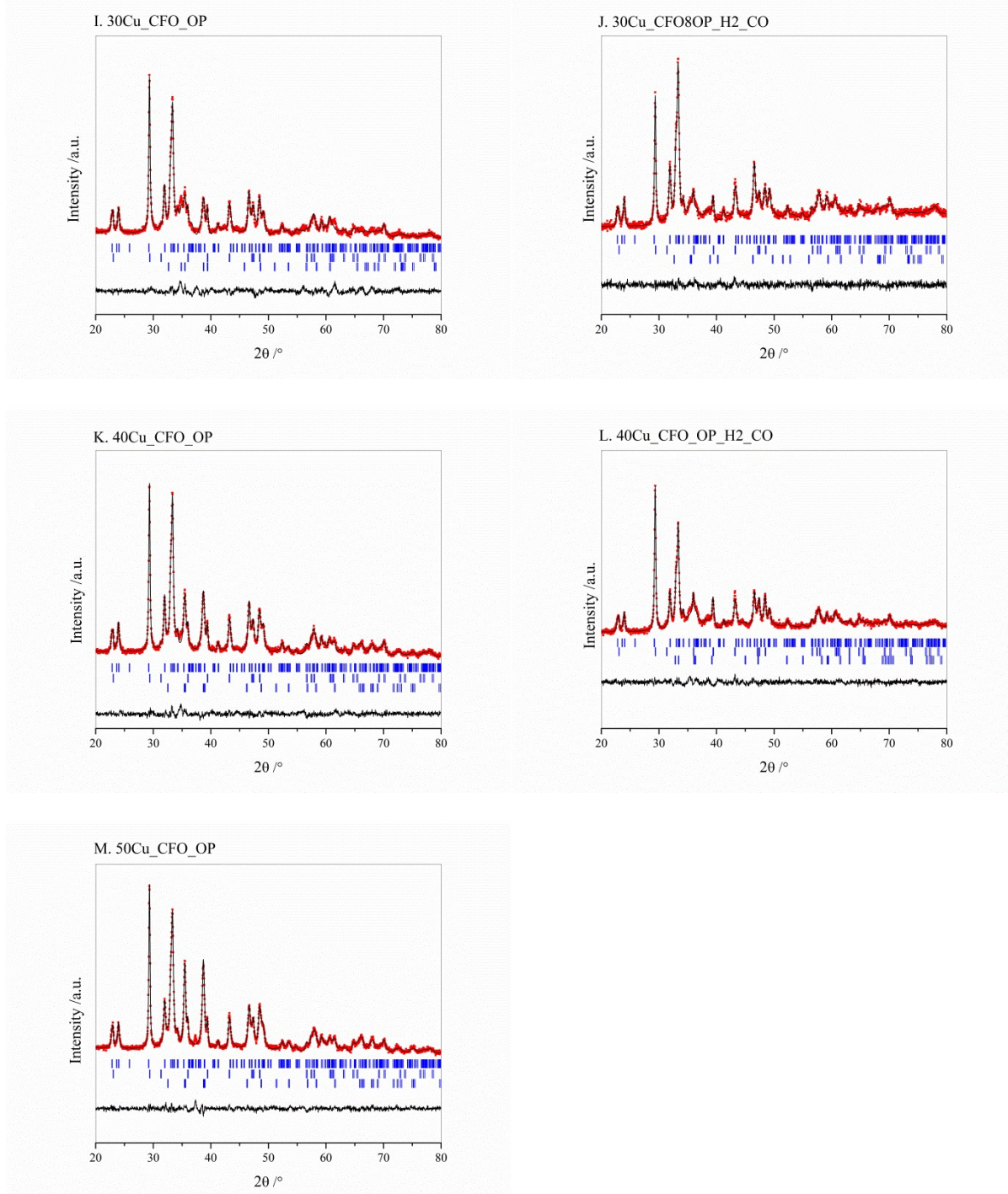


Figure SI 3 Observed, calculated and difference XRD patterns of: **A.** 1Cu-CFO_OP; **B.** 1Cu-CFO_OP after H₂ treatment and CO oxidation; **C.** 5Cu-CFO_OP; **D.** 5Cu-CFO_OP after H₂ treatment and CO oxidation; **E.** 10Cu-CFO_OP; **F.** 10Cu-CFO_OP after H₂ treatment and CO oxidation; **G.** 20Cu-CFO_OP; **H.** 20Cu-CFO_OP after H₂ treatment and CO oxidation; **I.** 30Cu-CFO_OP; **J.** 30Cu-CFO_OP after H₂ treatment and CO oxidation; **K.** 40Cu-CFO_OP; **L.** 40Cu-CFO_OP after H₂ treatment and CO oxidation; **M.** 50Cu-CFO_OP; results were refined in the *Pnma* space group in profile matching mode

together with appropriate space group describing secondary phase. Vertical bars are related to the calculated Bragg reflection position. Refined parameters are given in the Table S1.

X-Ray analysis of as-synthesized 40Cu-CFO_OP and after reaction, compared to reference compounds

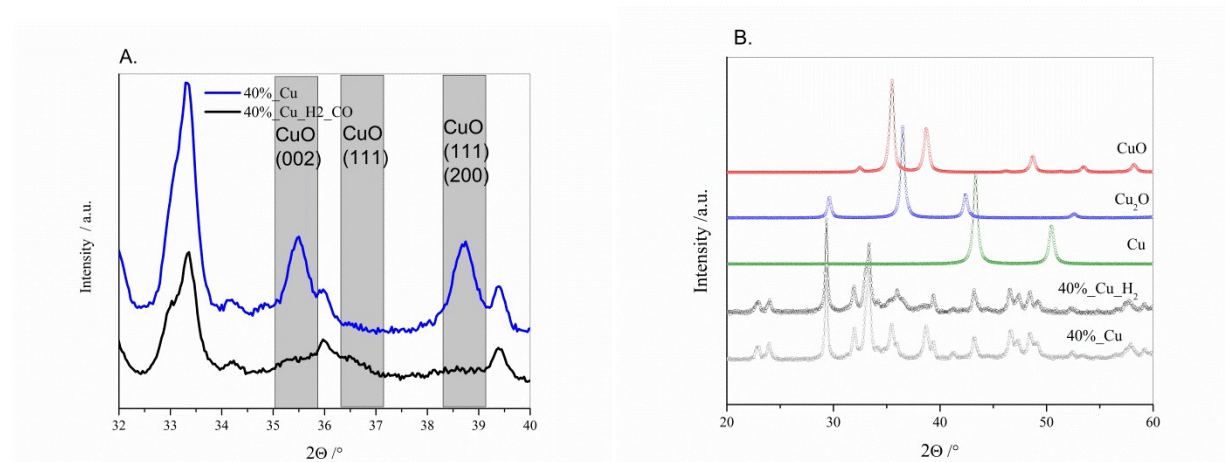


Figure SI 4A. X-Ray diffraction data in the 2θ region between 32° and 40° for as synthesized 40Cu-CFO_OP (blue line) and 40Cu-CFO_OP after H_2 treatment at 300°C followed by catalytic test at 400°C (black line). Grey boxes highlight the most intensive reflections belonging to the CuO phase (002) and (111)/(200) together with (111) reflection belonging to the Cu_2O phase; **B.** Observed XRD patterns for as synthesized 40Cu-CFO_OP (light grey) and 40Cu-CFO_OP after H_2 treatment at 300°C followed by catalytic test at 400°C (dark grey), stacked together with simulated XRD profile for Cu (green line), Cu_2O (blue line) and CuO (red line) phases. Simulations were performed in the Full Prof Package using profile broadening function determined for CuO phase in as-synthesized sample;

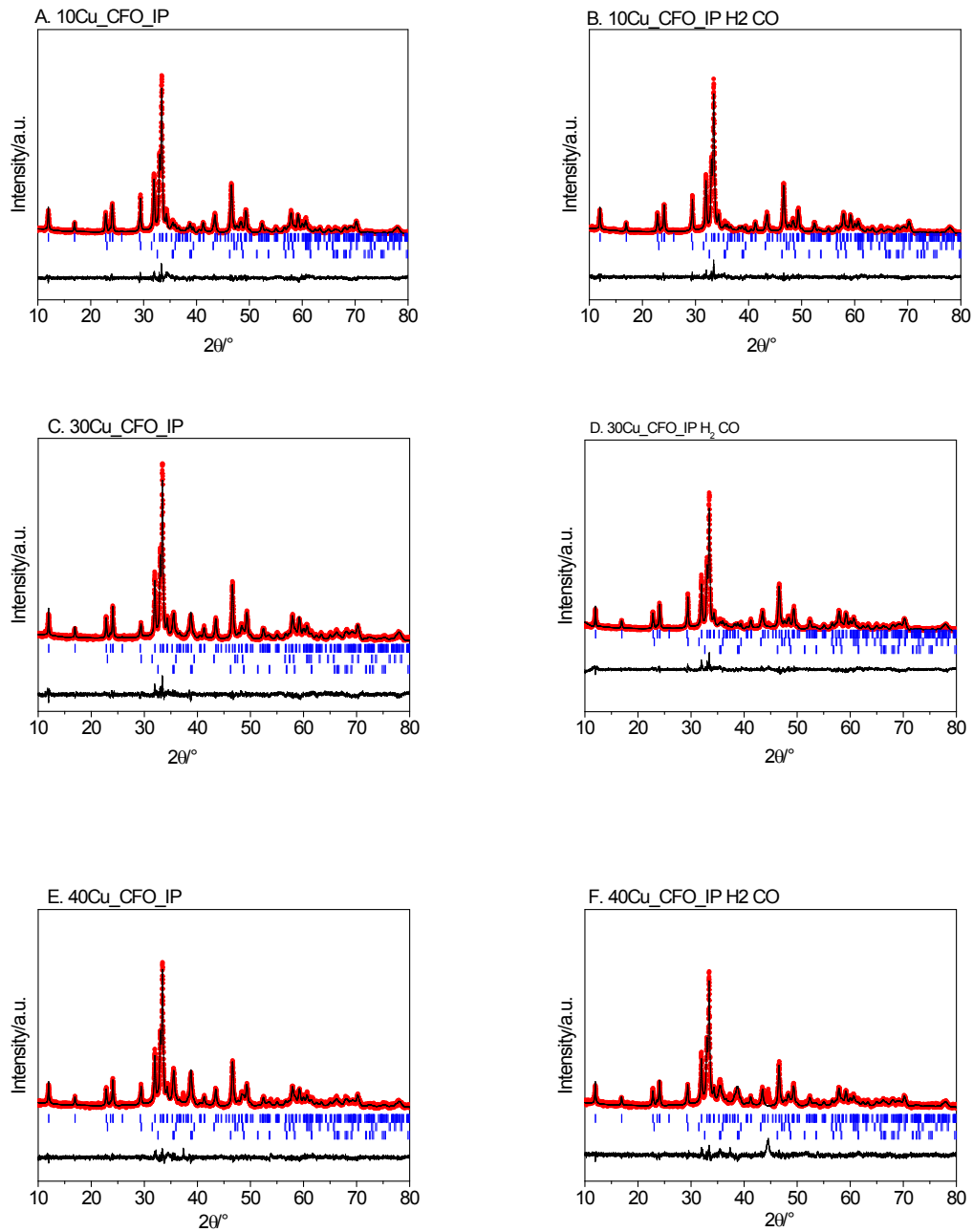
Lattice Parameter of impregnated samples

Table SI 3. Refined parameters corresponding to the XRD data presented in Fig. 2 for $x\text{Cu-CFO_IP}$ (where $10 < x < 40$), catalysts as synthesized and after CO oxidation.

Phase	Space Group	a [Å]	b [Å]	c [Å]	vol [Å³]	Phase fraction[%]
10 Cu-CFO_IP						
$\text{Ca}_2\text{Fe}_2\text{O}_5$	P n m a	5.42695(8)	14.7714(20)	5.6016(7)	449.037(107)	86.43(3.41)
CaCO_3	R -3 c	4.9978 (9)	4.9978 (9)	17.0583(41)	368.998(134)	9.41(66)
CuO	C 2/c	4.6853(14)	3.4219(8)	5.1122(16)	81.307(41)	4.17(39)

10 Cu-CFO_IP_CO						
Ca ₂ Fe ₂ O ₅	P n m a	5.4261(15)	14.7723(30)	5.6017 (14)	448.758(198)	86.24 (3.90)
CaCO ₃	R -3 c	4.9978 (9)	4.9978 (9)	17.0583(41)	368.998(134)	9.63(66)
CuO	C 2/c	4.6853(14)	3.4219(8)	5.1122(16)	81.307(41)	4.13(39)
10 Cu-CFO_IP_H2_CO						
Ca ₂ Fe ₂ O ₅	P n m a	5.4281 (8)	14.7722(23)	5.6021(9)	449.202(119)	87.65(3.71)
CaCO ₃	R -3 c	4.9978 (9)	4.9978 (9)	17.0583(41)	368.431(134)	9.77(0.72)
CuO	C 2/c	4.6853(14)	3.4219(8)	5.1122(16)	81.307(41)	2.58(0.39)
30 Cu-CF_IP						
Ca ₂ Fe ₂ O ₅	P n m a	5.4260 (5)	14.7704(8)	5.5954(3)	448.436(0.080)	85.16(3.53)
CaCO ₃	R -3 c	4.9978 (9)	4.9978 (9)	17.0583(41)	368.431(134)	3.03(0.55)
CuO	C 2/c	4.6853(14)	3.4219(8)	5.1122(16)	81.307(41)	11.81(0.60))
30 Cu-CFO_IP_CO						
Ca ₂ Fe ₂ O ₅	P n m a	5.4250(2)	14.7726(53)	5.5958(20)	447.786(280)	86.49(3.69)
CaCO ₃	R -3 c	4.9978 (9)	4.9978 (9)	17.0583(41)	368.431(134)	1.46(0.54)
CuO	C 2/c	4.6853(14)	3.4219(8)	5.1122(16)	81.307(41)	12.05(25)
30 Cu-CFO_IP_H2_CO						
Ca ₂ Fe ₂ O ₅	P n m a	5.4278 (5)	14.7704(14)	5.6017(5)	449.095(75)	86.49(3.74)
CaCO ₃	R -3 c	4.9978 (9)	4.9978 (9)	17.0583(41)	368.431(134)	10.79(0.78)
CuO	C 2/c	4.6853(14)	3.4219(8)	5.1122(16)	81.307(41)	2.72(0.40)
40 Cu-CFO_IP						
Ca ₂ Fe ₂ O ₅	P n m a	5.4242 (19)	14.7755(19)	5.5957(20)	448.470(0.095)	78.83(1.29)
CaCO ₃	R -3 c	4.9978 (9)	4.9978 (9)	17.0583(41)	368.431(134)	4.51(0.05)
CuO	C 2/c	4.6853(14)	3.4219(8)	5.1122(16)	81.307(41)	16.66(0.17)
40 Cu-CFO_IP_CO						
Ca ₂ Fe ₂ O ₅	P n m a	5.4276 (8)	14.7746(22)	5.5992(8)	449.009114)	76.20(2.01)
CaCO ₃	R -3 c	4.9978 (9)	4.9978 (9)	17.0583(41)	368.431(134)	5.61(0.72)
CuO	C 2/c	4.6853(14)	3.4219(8)	5.1122(16)	81.307(41)	18.19(1.24)
40 Cu-CFO_IP_H2_CO						
Ca ₂ Fe ₂ O ₅	P n m a	5.4285(4)	14.7711(11)	5.6005(4)	449.078(0.111)	78.71(1.56)
CaCO ₃	R -3 c	4.9978 (9)	4.9978 (9)	17.0583(41)	368.431(134)	5.33(0.60)
CuO	C 2/c	4.6853(14)	3.4219(8)	5.1122(16)	81.307(41)	15.96(0.82)
CuO						
CuO	C 2/c	4.69151(31)	3.43179(26)	5.13881(32)	81.609(10)	100(0) 6.04
CFO						
Ca ₂ Fe ₂ O ₅	P n m a	5.43302(52)	14.78038(144)	5.60496(54)	450.090(75)	100(0) 1.22

Figure SI 5 XRD pattern of impregnated samples as-synthesized and after reaction



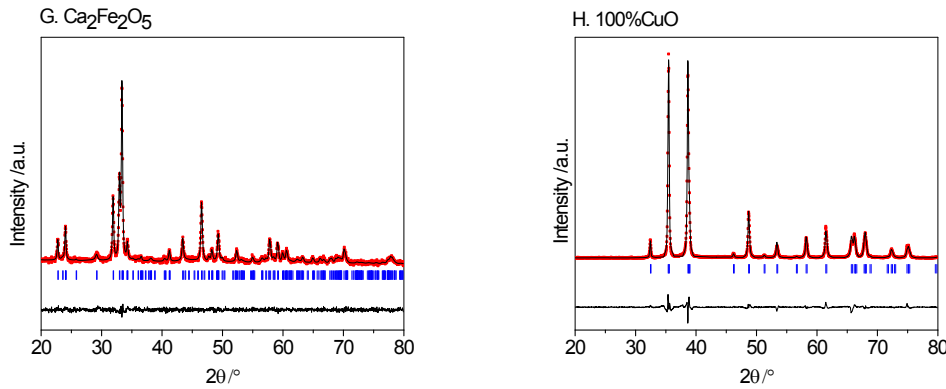


Figure SI 5 Observed, calculated and difference XRD patterns of: **A.** 10Cu-CFO_IP; **B.** 10Cu-CFO_IP after H_2 treatment and CO oxidation; **C.** 30Cu-CFO_IP; **D.** 30Cu-CFO_IP after H_2 treatment and CO oxidation; **E.** 40Cu-CFO_IP; **F.** 40Cu-CFO_IP after H_2 treatment and CO oxidation; **G.** as-synthesized pure $\text{Ca}_2\text{Fe}_2\text{O}_5$ **H.** pure CuO. Results were refined in the *Pnma* space group in profile matching mode together with appropriate space group describing secondary phase. Vertical bars are related to the calculated Bragg reflection position. Refined parameters are given in the Table SI 3.

EXAFS fit parameters

Table SI 4 EXAFS fit parameters with S_0^2 -passive electron reduction factor, ΔE_0 -energy shift, R-internuclear distance, σ^2 -mean squared displacement.

T (°C)	30Cu-CFO_OP	Bond	Site	S_0^2	ΔE_0 (eV)	R (Å)	σ^2 (Å ²)	R_Factor	
RT/Air	$\text{Ca}_2\text{Fe}_2\text{O}_5$	Cu-O	(1)	1.24±0.13	-0.10±1.96	1.977±0.002	0.011±0.002	0.010	
		Fe-O ₁	O_{h1}	0.45±0.11	-4.25±3.96	1.968±0.017	0.004±0.002	0.010	
		Fe-O ₂	O_{h2}	0.45±0.11	-4.25±3.96	2.115±0.017	0.005±0.002	0.010	
		Fe-O ₂	T_{d1}	0.45±0.11	-4.25±3.96	1.863±0.013	0.004±0.002	0.010	
		Fe-O ₃	T_{d2}	0.45±0.11	-4.25±3.96	1.904±0.013	0.004±0.002	0.010	
300°C/ H_2	$\text{Ca}_2\text{Fe}_2\text{O}_5$	Cu-Cu	(1)	0.83±0.09	3.63±0.73	2.534±0.003	0.015±0.001	0.011	
		Fe-O ₁	O_{h1}	0.47±0.14	-5.01±4.44	1.968±0.017	0.006±0.003	0.014	
		Fe-O ₂	O_{h2}	0.47±0.14	-5.01±4.44	2.115±0.017	0.008±0.007	0.014	
		Fe-O ₂	T_{d1}	0.47±0.14	-5.01±4.44	1.863±0.024	0.006±0.003	0.014	
		Fe-O ₃	T_{d2}	0.47±0.14	-5.01±4.44	1.904±0.024	0.006±0.003	0.014	
200°C/ CO/O_2	$\text{Ca}_2\text{Fe}_2\text{O}_5$	Cu ₂ O	Cu-O	(1)	0.27±0.05	-0.63±2.01	1.864±0.013	0.001±0.002	0.008
		Fe-O ₁	O_{h1}	0.45±0.13	-3.09±4.31	1.968±0.021	0.005±0.003	0.002	
		Fe-O ₂	O_{h2}	0.45±0.13	-3.09±4.31	2.115±0.021	0.004±0.005	0.002	
		Fe-O ₂	T_{d1}	0.45±0.13	-3.09±4.31	1.863±0.013	0.018±0.003	0.002	
		Fe-O ₃	T_{d2}	0.45±0.13	-3.09±4.31	1.904±0.013	0.018±0.003	0.002	
T (°C)	40Cu-CFO_OP	Bond	Site	S_0^2	ΔE_0 (eV)	R (Å)	σ^2 (Å ²)	R_Factor	
RT/Air	$\text{Ca}_2\text{Fe}_2\text{O}_5$	Cu-O	(1)	1.27±0.11	-1.12±0.57	1.961±0.009	0.010±0.002	0.007	
		Fe-O ₁	O_{h1}	0.45±0.12	-1.98±4.68	1.968±0.018	0.005±0.002	0.002	
		Fe-O ₂	O_{h2}	0.45±0.12	-1.98±4.68	2.115±0.018	0.005±0.008	0.002	
		Fe-O ₂	T_{d1}	0.45±0.12	-1.98±4.68	1.863±0.017	0.005±0.002	0.002	
		Fe-O ₃	T_{d2}	0.45±0.12	-1.98±4.68	1.904±0.017	0.005±0.002	0.002	

	Cu	Cu-Cu	(1)	0.83±0.09	3.63±0.73	2.534±0.002	0.014±0.001	0.011
300°C/H ₂	Ca ₂ Fe ₂ O ₅	Fe-O ₁	<i>O_{h1}</i>	0.47±0.17	-4.29±5.27	1.968±0.021	0.006±0.003	0.001
		Fe-O ₂	<i>O_{h2}</i>	0.47±0.17	-4.29±5.27	2.115±0.021	0.010±0.009	0.001
		Fe-O ₂	<i>T_{d1}</i>	0.47±0.17	-4.29±5.27	1.863±0.026	0.006±0.003	0.001
		Fe-O ₃	<i>T_{d2}</i>	0.47±0.17	-4.29±5.27	1.904±0.026	0.006±0.003	0.001
		Cu ₂ O	Cu-O	(1)	0.27±0.05	-0.02±1.81	1.851±0.004	0.001±0.002
200°C/ CO/O ₂	Ca ₂ Fe ₂ O ₅	Fe-O ₁	<i>O_{h1}</i>	0.46±0.13	-3.80±4.23	1.968±0.015	0.004±0.002	0.001
		Fe-O ₂	<i>O_{h2}</i>	0.46±0.13	-3.80±4.23	2.115±0.015	0.004±0.005	0.001
		Fe-O ₂	<i>T_{d1}</i>	0.46±0.13	-3.80±4.23	1.863±0.021	0.004±0.002	0.001
		Fe-O ₃	<i>T_{d2}</i>	0.46±0.13	-3.80±4.23	1.904±0.021	0.004±0.002	0.001

Fourier Transformation of the EXAFS signal of 30Cu-CFO_OP at the Cu edge

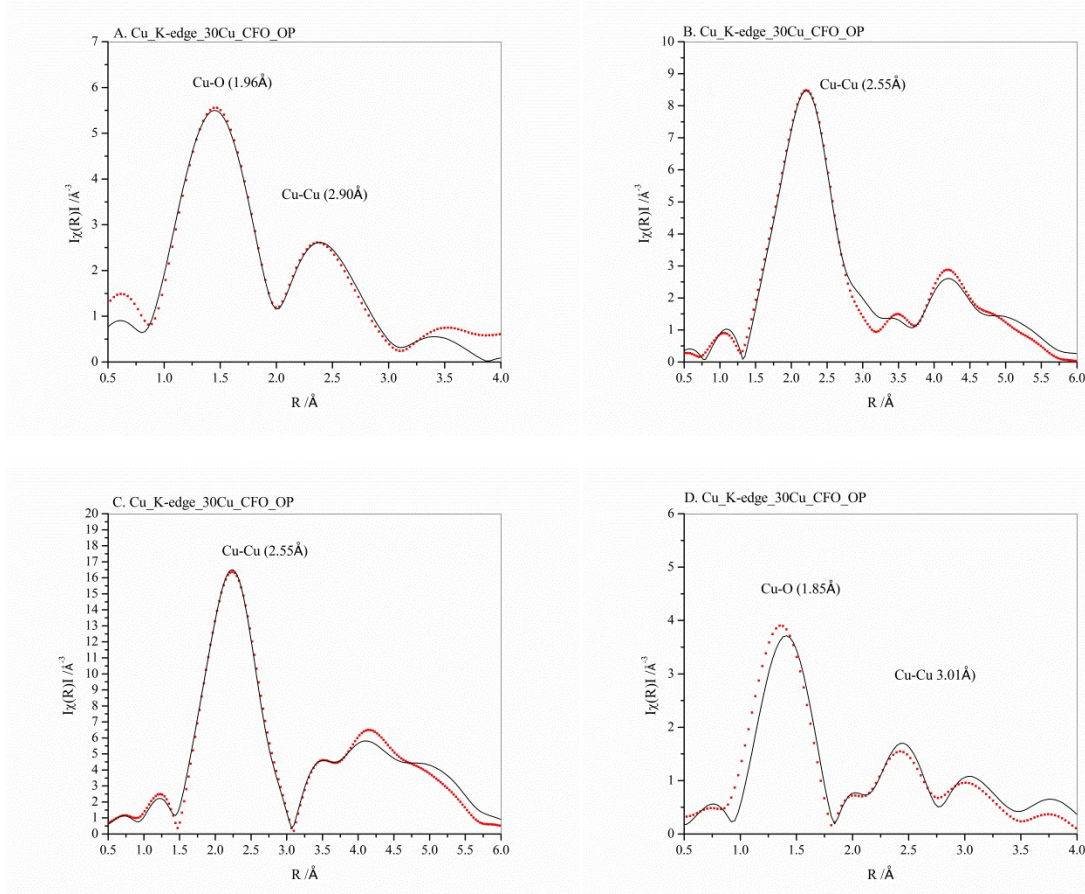


Figure SI 6 Experimental k^3 -weighted FT of the $\xi(k)$ function together with the best fit for 30Cu-CFO_OP measured at the Cu K-edge under **A.** Air at RT, **B.** H_2 at 300°C , **C.** He at RT and **D.** CO/O_2 at 200°C .

Fourier Transformation of the EXAFS signal of 30Cu-CFO_OP at the Fe-edge

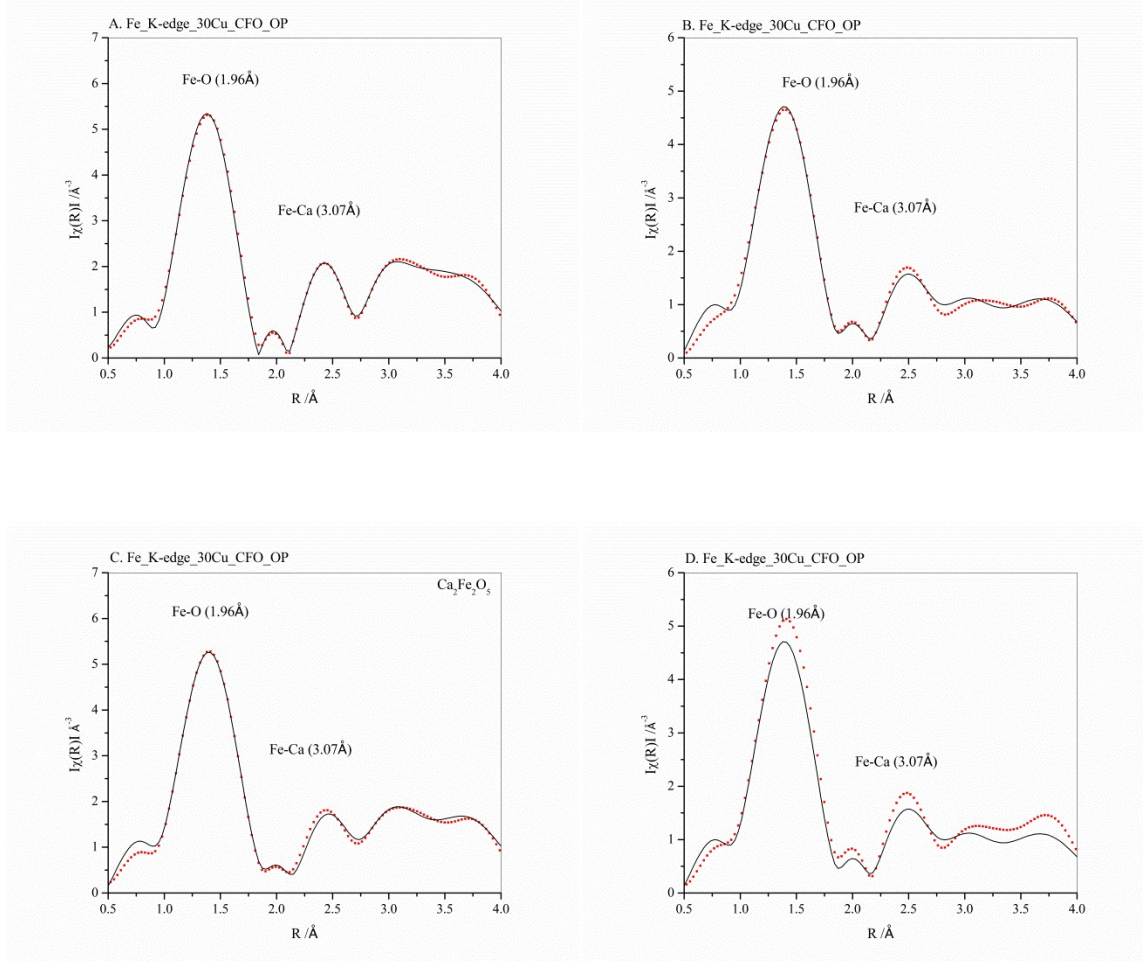


Figure SI 7 Experimental k^3 -weighted FT of the $\xi(k)$ function together with the best fit for 30Cu-CFO_OP measured at the Fe K-edge under **A.** Air at RT, **B.** H_2 at 300°C , **C.** He at RT and **D.** CO/O_2 at 200°C .

Fourier Transformation of the EXAFS signal of 40Cu-CFO_OP at the Cu-edge

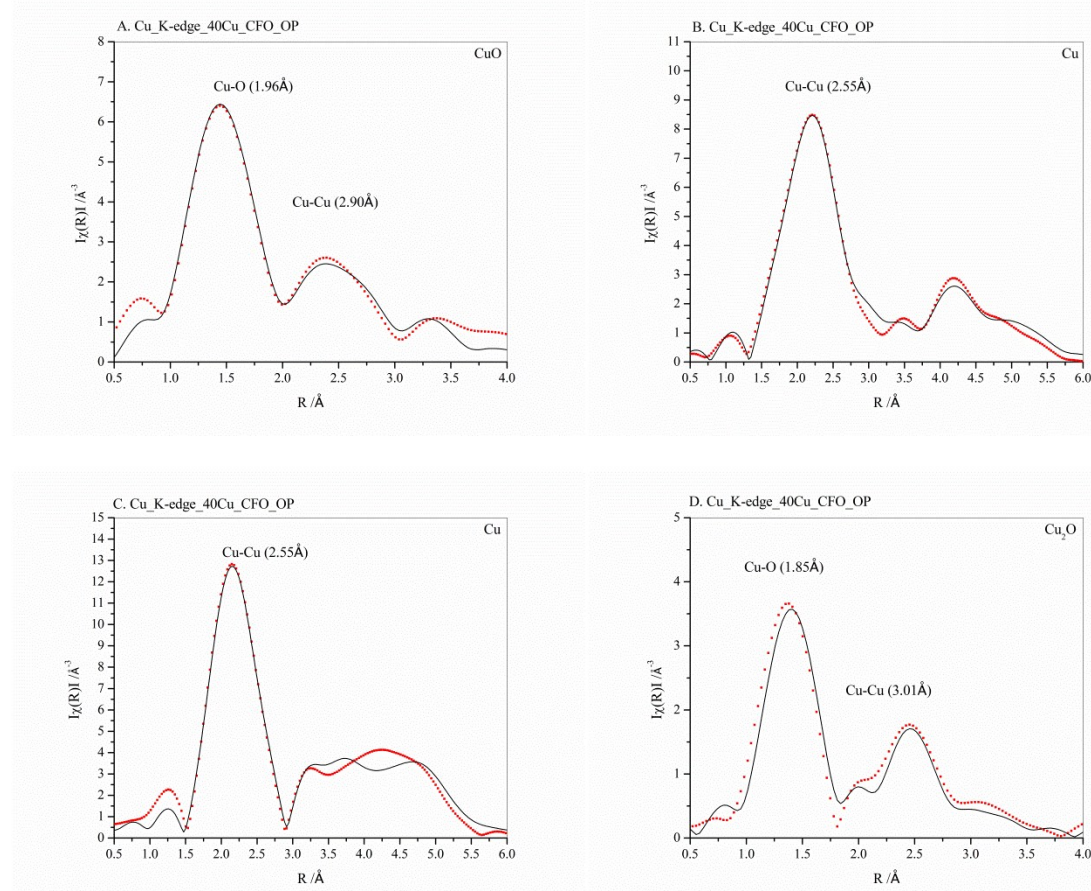
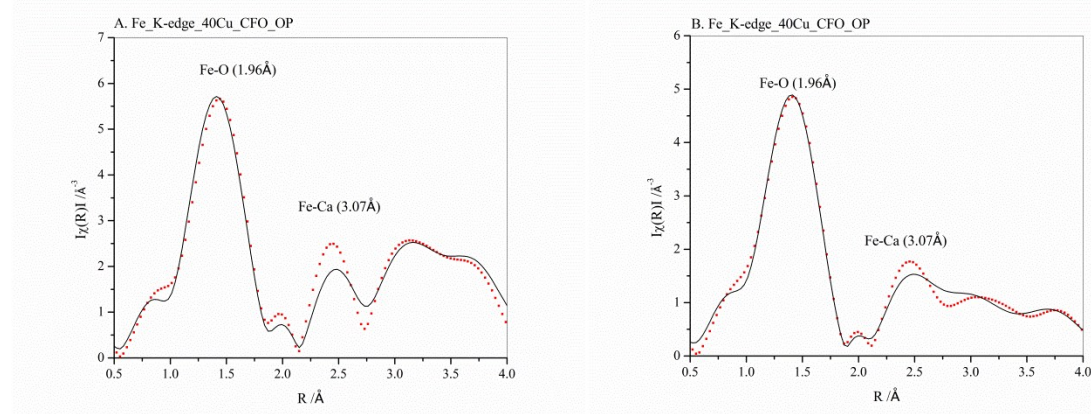


Figure SI 8 Experimental k^3 -weighted FT of the $\xi(k)$ function together with the best fit for 40Cu-CFO_OP measured at the Cu K-edge under **A.** Air at RT, **B.** H₂ at 300°C, **C.** He at RT and **D.** CO/O₂ at 200°C.

Fourier Transformation of the EXAFS signal of 40Cu-CFO_OP at the Fe-edge



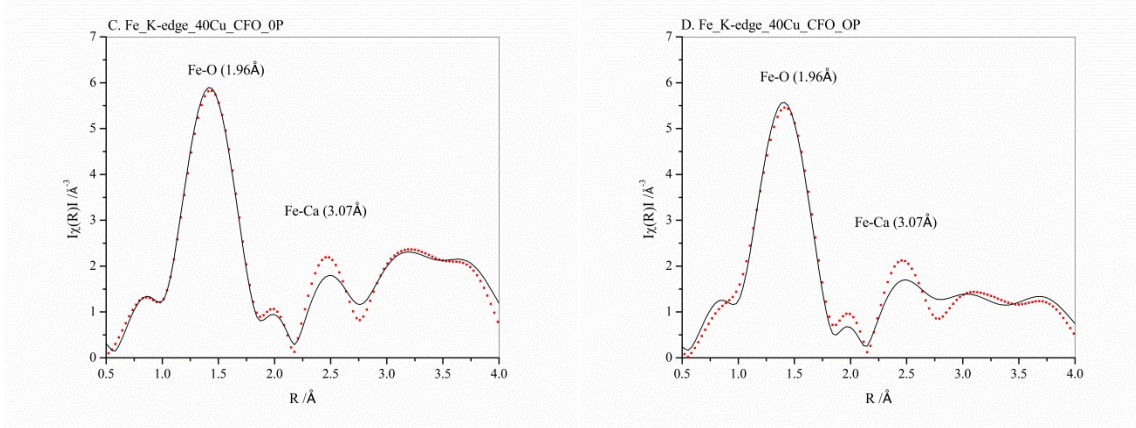


Figure SI 9 Experimental k^3 -weighted FT of the $\xi(k)$ function together with the best fit for 40Cu-CFO_OP measured at the Fe K-edge under **A.** Air at RT, **B.** H₂ at 300°C, **C.** He at RT and **D.** CO/O₂ at 200°C.

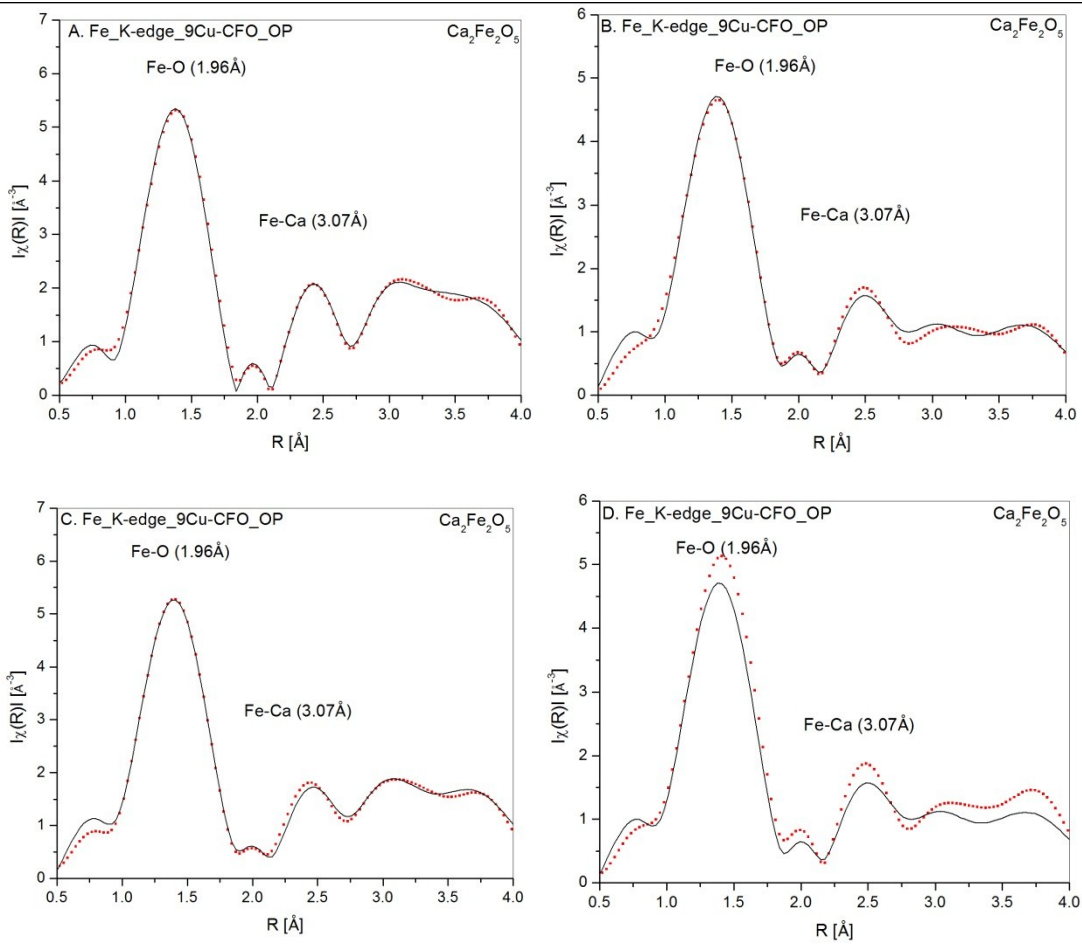


Figure SI 10 Experimental k^3 -weighted FT of the $\xi(k)$ function together with the best fit for 40Cu-CFO_OP measured in the Fe K-edge under: **A.** Air at RT; **B.** H₂ at 300°C; **C.** He at RT; **D.** CO/O₂ at 200°C.

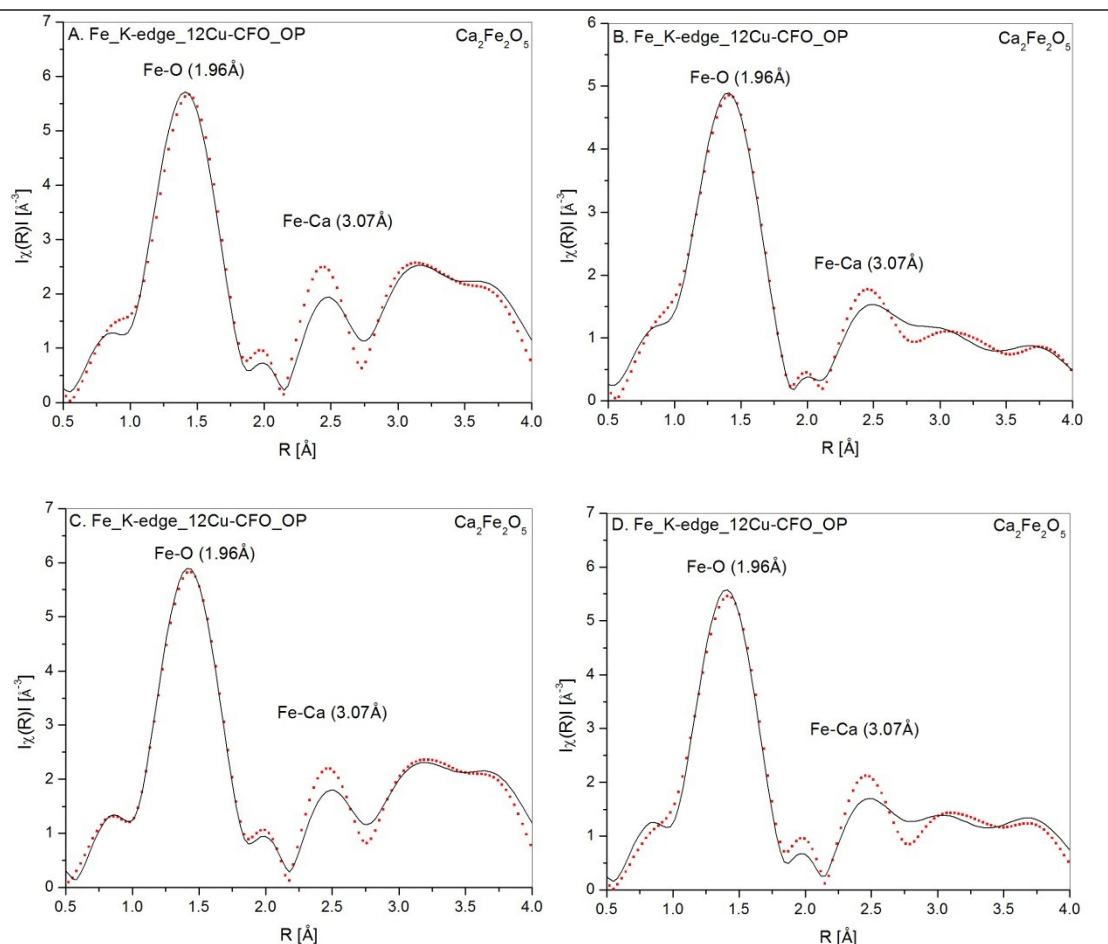


Figure SI 11 Experimental k^3 -weighted FT of the $\xi(k)$ function together with the best fit for 12Cu-CFO_OP measured in the Fe K-edge under: **A.** Air at RT; **B.** H_2 at 300°C ; **C.** He at RT; **D.** CO/O_2 at 200°C .